

# Characterization of Pore Structure of Nuclear Grade Graphite Using Image Analysis Technique and Mercury Porosimetry

Eung-Seon Kim\*, Ji-Seon Song, Sung-Deok Hong

Korea Atomic Energy Research Institute, 1045 Daedeok-daero, Yuseong-gu, Daejeon, 305-353

\*Corresponding author: kimes@kaeri.re.kr

## 1. Introduction

In a very high temperature reactor, graphite core components are stressed due to dimensional change and irradiation creep so that the integrity of the graphite component must be accessed by evaluating the cracking and failure of graphite [1]. Normally polycrystalline graphite fails through a crack initiation induced by stress/inherent flaw, sub-critical crack growth from pore to pore and final propagation of a critical defect [2]. Consequently, the information on the pore structure is inevitably necessary to understand and model the fracture behavior of nuclear graphite. In this study, the pore structures of commercially available nuclear graphites were investigated using an optical image analysis method and mercury porosimetry.

## 2. Experiments

### 2.1 Materials

Five grades of nuclear graphite were used in this study: IG-110 (petroleum coke, isostatically molded) and IG-430 (pitch coke, isostatically molded) produced by the Toyo Tanso Co, Ltd, Japan, NBG-17 (pitch coke, vibrationally molded) and NBG-25 (petroleum coke, isostatically molded) produced by the SGL Carbon Group, Germany and PCEA (petroleum coke, extruded) produced by the Graftech. The main properties of the graphites are summarized in Table 1.

Table 1. Typical properties of the nuclear graphites

Grade	Density (g/cm <sup>3</sup> )	Coke particle size (μm)
IG-110	1.78	20
IG-430	1.82	10
NBG-17	1.84	Max. 900
NBG-25	1.81	Max. 60
PCEA	1.83	Max. 360

### 2.2 Optical Image Analysis

Samples were mounted using a vacuum-impregnation apparatus (Struers, EpoVac) to fill most accessible pores with epoxy resin and thus maintain the original structure of the graphite. The sample mounts were ground up to P4200 grit SiC paper and finally polished on a high napped cloth using 0.05 μm alumina powder.

The optical pore structure was quantitatively examined using image analysis software (SARAMSOFT Co., Ltd., ImagePartner) coupled with an Olympus

GX51 polarized light optical microscope. The composited images were larger than 10 times the maximum particle size in width and length, respectively. The acquired composite images were converted to monochromatic 8 bits grayscale and filtered. The individual pores on the image were identified and digitally filled by adjusting the range of grey nuances based on the histogram.

### 2.3 Mercury Porosimetry

Fundamental porosity parameters such as pore size distribution pore volume and pore surface area were determined by mercury porosimetry measurements (Micromeritics Instrument Corporation, Mercury Porosimeter, Model AutoPore IV 9500). Pressures were increased up to 60,000 psi, corresponding to a pore size of 3 nm.

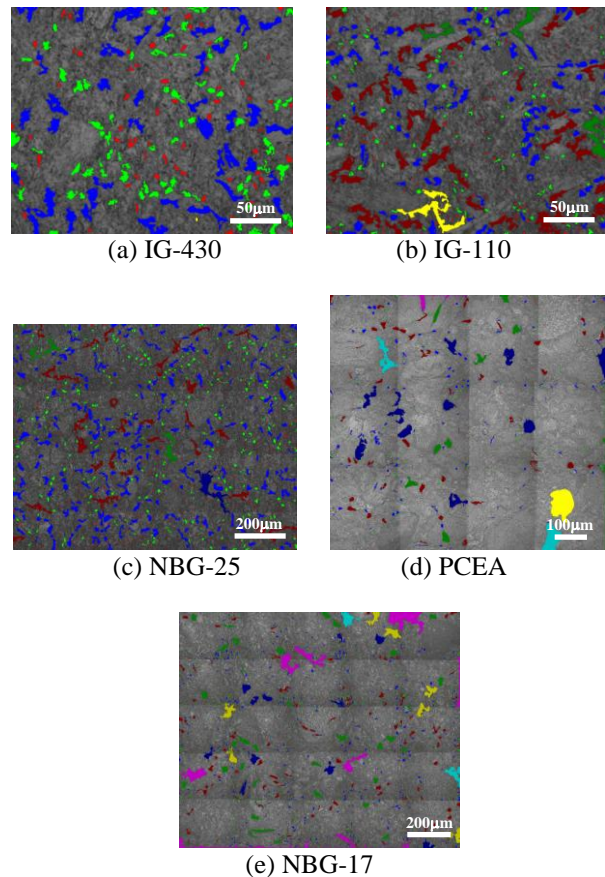


Fig. 1. Composited images and digitally filled pore structures of the nuclear graphites.

### 3. Results and Discussion

#### 3.1 Optical Pore Structure

Fig. 1 shows optical pore structures of the composited images. The open and closed pore was discernible by small differences in their grey tones. Closed pores or cracks formed by volumetric shrinkage during calcinations in the filler particles were known to be parallel to the basal planes. Two types of open pore were identified within the binder phases. One is gas entrapment pores formed during the mixing and baking stage of manufacture. The other is narrow, slit-shaped pores formed as a result either volumetric shrinkage on baking or of anisotropic contraction on cooling from graphitization temperatures. They are often found at domain/mosaic boundaries in the binder phase and frequently connected to gas entrapment pores.

The size distribution of optical pores is shown Fig. 2. Generally, as the filler coke particle size increased the larger pores with low percentage were observed. However the pores of 7 ~ 15  $\mu\text{m}$  in diameter were predominant regardless of the grade.

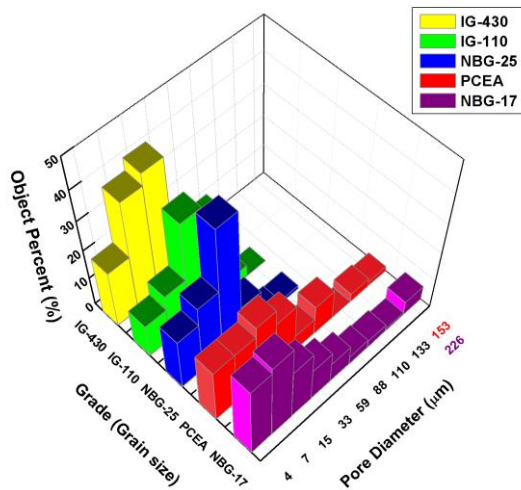


Fig. 2. Optical pore size distribution of the nuclear graphites.

#### 3.2 Pore Size Distribution Measured by Mercury Porosimetry

Fig. 3 shows the pore size distribution of the nuclear graphites measured by mercury porosimetry. The pore entrance diameter ranged from 3 nm to 400  $\mu\text{m}$ . Mercury porosimetry measurements showed large difference in the pore spectra between the fine-grained and the medium-grained nuclear graphites. The major pores in the fine-grained graphites (IG-430, IG-110 and NBG-25) were concentrated at about 2~5  $\mu\text{m}$ . The distribution of pore size in the medium-grained graphites (PCEA and NBG-17) was relatively broad and the major pores were concentrated at about 10~50  $\mu\text{m}$ .

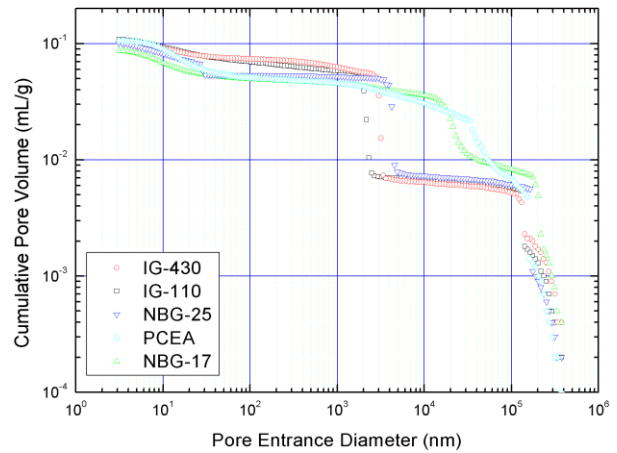


Fig. 3. Pore entrance diameters vs. cumulative pore volume of the nuclear graphites.

### 4. Summary

Image analysis is useful method to gain direct information on pore size distribution and pore shape (aspect ratio) of nuclear graphite. However the observable pore size may be limited to micron-scale depending on the magnification of a microscope and quality of sample preparation.

The pore size calculated by mercury porosimetry is not truly indicative of the real pore size due to the approximate assumptions (circular pore and constant values for the surface tension and contact angle of mercury), however it can effectively compare the quantitative porosity parameter of the nuclear graphite from nano- to micro-scale.

Each method has its own bias so that two methods should be used complementarily to clearly understand the pore structure of the nuclear graphites.

### ACKNOWLEDGEMENT

This study has been carried out under the Nuclear R & D Program supported by the Korean Ministry of Education, Science and Technology.

### REFERENCES

- [1] S. Ishiyama, T. D. Burchell, J. P. Strizak and M. Eto, J. Nucl. Mater. Vol.230, pp.1, 1996
- [2] T. D. Burchell, Carbon, Vol.34, pp.297, 1996
- [3] N. Murdie, I. A. S. Edwards and H. Marsh, Carbon, Vol.24, pp.267, 1986